

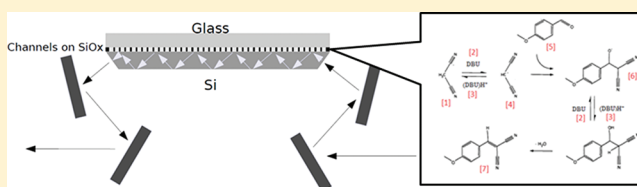
Attenuated Total Reflection-Infrared Nanofluidic Chip with 71 nL Detection Volume for *in Situ* Spectroscopic Analysis of Chemical Reaction Intermediates

Engin Karabudak,^{*,†,‡} Barbara L. Mojet,[§] Stefan Schlautmann,[‡] Guido Mul,[†] and Han J. G. E. Gardeniers[‡]

[†]Photo Catalytic Synthesis Group, [‡]Mesoscale Chemical Systems group, and [§]Catalytic Processes and Materials and MESA+ Institute for Nanotechnology, University of Twente, P.O. Box 217, 7500 AE Enschede, The Netherlands

Supporting Information

ABSTRACT: We present a micromachined silicon attenuated total reflection-infrared (ATR-IR) crystal with integrated nanofluidic glass channels which enables infrared spectroscopic studies with only 71 nL sample volume. Because of the short path length through silicon, the system allows IR spectroscopy down to 1200 cm^{-1} , which covers the typical fingerprint region of most organic compounds. To demonstrate proof-of-principle, the chip was used to study a Knoevenagel condensation reaction between malononitrile and *p*-anisaldehyde catalyzed by different concentrations of 1,8-diazabicyclo[5.4.0]undec-7-ene (DBU) in solvent acetonitrile. By *in situ* measurement, it was demonstrated for the first time that at certain concentrations of DBU, reaction intermediates become stabilized, an effect that slows down or even stops the reaction. This is thought to be caused by increased ionic character of the solvent, in which protonated DBU stabilizes the intermediates. This clearly demonstrates that infrared mechanistic studies of chemical reactions are feasible in volumes as little as 71 nL.



An important trend in modern analytical chemistry is the development of instrumentation to identify chemical species in the smallest possible sampling volume.¹ This is particularly relevant for developments in the upcoming field of nanofluidics, with extremely low sample volumes in the range of nanoliters, picoliters, and in some cases even femtoliters.² Nanofluidics, with promising applications in chemistry and biology^{3,4} focuses not only on the accurate handling of extremely small amounts of liquids but also fosters the notion that the behavior of liquids in confinement is fundamentally different.^{3–6} Current nanofabrication technology allows us to manufacture experimental model systems, with dimensions close to the mesopores in porous materials of interest in chemical engineering or comparable to filamental structures relevant in biology. State-of-the-art nano and microtechnology also allows the integration of analytical elements that are scalable to the relevant nanostructural dimensions or, better still, scalable to the range of the physicochemical phenomena occurring in or on these nanostructures.

Infrared (IR) spectroscopy is an important tool to study mechanistic properties of chemical reactions.⁷ Attenuated total reflection-infrared (ATR-IR) spectroscopy is an emerging technique to study chemistry in the liquid phase or to identify the interactions of solids with liquids, relevant for determination of, e.g., sorption equilibria. The advantage of ATR spectroscopy as compared to transmission spectroscopy lies in the short penetration depth of light into the sample, which amounts to at most a few micrometers, beneficial for strongly absorbing media such as water or solids.⁸ In the application of ATR spectroscopy for mechanistic studies in chemistry or

catalysis, using chemicals like isotopes or special intermediates can be advantageous to assist in identification of the species causing certain infrared absorptions as well as to investigate the underlying mechanism of liquid phase reactions.⁹ The isotopes and the intermediates, but often also the compounds themselves, can be expensive and difficult to get in sufficient amounts. One trivial way of performing mechanistic studies with expensive chemicals is to reduce the sampling size. To downsize the sample amounts required for ATR spectroscopy, several examples exist in the literature of combining ATR-IR with microfluidic systems.^{10–13}

In a recent publication, an array of nanofluidic channels implemented on a silicon ATR crystal was reported,¹⁴ with a design in which the periodicity of the nanochannels was kept below the wavelength of infrared light in order to minimize light scattering at the optical grating that was created by the regular array of nanofluidic channels. Here, in order to decrease scattering, we use a design with a nanofluidic channel periodicity ($30\ \mu\text{m}$) far above the wavelength of the infrared light ($1.5\text{--}10\ \mu\text{m}$). In addition, the chosen channel height ($600\ \text{nm}$) is in close proximity to the penetration depth of the evanescent field of the ATR-IR light, which enables us to probe the entire volume of the reaction chamber. Finally, for ATR measurements with Si crystals, a cutoff wavenumber of $1500\ \text{cm}^{-1}$ is common,⁸ but by decreasing the path length of infrared light through Si as a result of the thin substrate,¹⁰ we were able

Received: November 1, 2011

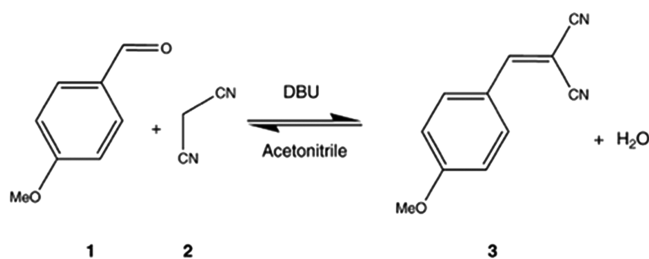
Accepted: February 16, 2012

Published: February 16, 2012

to measure down to a wavenumber of 1200 cm^{-1} . This makes it possible to approach the typically very specific IR fingerprint region as it is known for most organic compounds. The use of nanochannels which will be uniformly filled with a liquid sample by capillary forces also has advantages in terms of reproducibility, compared to a method in which a drop of a few microliters of sample is positioned on the surface of an ATR crystal (see Figure SI-16 in Supporting Information), in particular if polarity changes occur during a reaction.

As proof-of-principle of the device, we have investigated the mechanism of a Knoevenagel condensation reaction, in particular the reaction that is shown in Scheme 1: *p*-

Scheme 1. Investigated Knoevenagel Condensation Reaction: *p*-Anisaldehyde Reacts with Malononitrile to PMB and Water, A Reaction That Is Catalyzed by DBU



anisaldehyde reacts with malononitrile to form 2-[(4-methoxyphenyl)methylidene]propanedinitrile (PMB) and water. This reaction was previously studied in microfluidic chips with much larger channels, in the range of several tens of micrometers width and height, using off-line UV-vis spectroscopy¹⁵ and online Raman spectroscopy¹⁶ for analysis.

Note that the small volume of the developed ATR-IR cell is not only beneficial for reducing consumption of expensive chemicals as mentioned above or for studying the effects of confinement, it also allows connection of the cell in-line with analytical equipment like chromatography columns of all sorts, for which IR absorption spectroscopy may be a relevant hyphenation technique.¹⁷ Analytical equipment development has been driven quite significantly by miniaturization over the last decades, and in particular miniaturized detection elements have been a popular topic, see, e.g., the work of Ogburn et al. on an electrochemical detector with an effective detection volume of 20 nL, which was recently published in this journal.¹⁸ A detection volume of 71 nL is in the range of what one would typically find in commercial micro-LC applications ($\sim 100\text{ nL}$ for UV-vis cells).

EXPERIMENTAL SECTION

Fabrication of Nanofluidic ATR-IR Chip. Conventional Si microfabrication methods were used to manufacture an ATR-IR chip from a {100} silicon wafer with a 600 nm SiO_2 layer (formed by thermal oxidation of silicon in steam at $1150\text{ }^\circ\text{C}$), to which a glass wafer was anodically bonded after reservoir structures and access holes had, respectively, been powder-blasted and etched. A total of 300 nanochannels with a depth of 600 nm, a width of $30\text{ }\mu\text{m}$, and a length of 1 cm had been etched into the SiO_2 layer on the silicon wafer before the bonding process. The nanochannels had a pitch, i.e., the center-to-center distance of the channels, of $40\text{ }\mu\text{m}$. Two microchannels, $300\text{ }\mu\text{m}$ wide and $3\text{ }\mu\text{m}$ deep, were etched in the glass wafer and served as filling inlets/outlets for the nanochannels (see Figure SI-9 in Supporting Information). Because the microchannels are in the glass wafer, they do not interfere with the evanescent IR light and hence do not affect the IR spectra (see Figure SI-15 in Supporting Information). Anisotropic etching of the single-crystalline silicon in KOH yielded 54.7° slopes corresponding to the {111} slow-etching crystal planes.¹⁰ The total size of the chip is 2.5 cm by 1.5 cm, which means that 13 of these chips can be produced from one 4 in. silicon wafer. Details of the fabrication procedure can be found in the Supporting Information.

ATR Holder Construction/IR Spectroscopy. The setup consists of four mirrors and a chip holder (see Figure SI-14 in Supporting Information) that are placed in an IR spectrometer, type Vertex 70, from Bruker Optics. A beam aperture of 8 mm, a spectral resolution of 4 cm^{-1} , and an integration time of 3 s were chosen for the measurements. A measurement on an empty chip served as the background signal for all measurements. The mirrors focus an IR beam on the {111} side faces of the silicon chip. The holder also has fluidic inlets for resealable capillary connections from Upchurch (Nanoport connections). The nanofluidic channel height is 600 nm, for which dimension no confinement effects, as mentioned in the recent literature,^{19,20} are expected. The penetration depth of the evanescent part of the internally reflected IR light is nearly equal to the height of the channels so that a significant volume of the nanofluidic channels is sampled by the IR beam. Channel filling is visible by the naked eye. The ATR-IR chip (see Figure 1) only needs 71 nL of sample volume, while the obtained IR signal is that good that one can get a complete spectrum in just 3 s.

IR Penetration Depth. Infrared light propagates inside the Si part of the chip by attenuated total reflection. The IR beam hits the side of the chip (as shown in Figure 1) with a spot size of 1 cm diameter, which ensures coverage of the complete

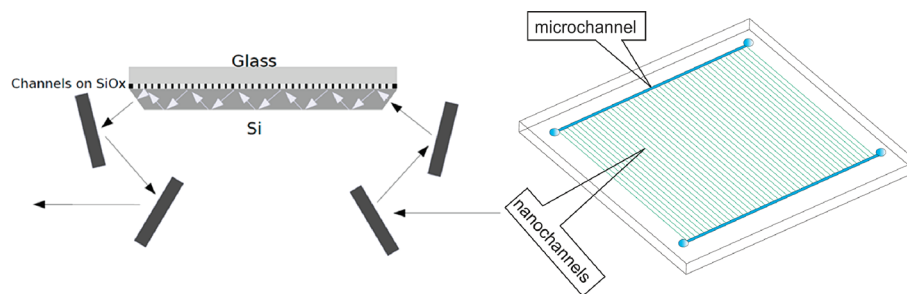


Figure 1. (Left) cross-section of the nanofluidic chip showing the ATR-IR setup and trajectory of IR light; (right) schematic drawing of the nanofluidic channel chip.

nanochannel length (note that the nanochannels are aligned perpendicular to the direction of the beam, Figure 1). Since the thickness of the Si part is $530\ \mu\text{m}$, 7 internal so-called "bounces" will occur, i.e., the Si surface is sampled at 7 specific locations (see Figure SI-16 in Supporting Information for an artist impression).

The penetration depth of the IR light can be calculated from

$$d_p = \frac{\lambda}{n_{\text{Si}}} \frac{1}{2\pi \sqrt{\sin^2 \theta - \left(\frac{n_{\text{ACN}}}{n_{\text{Si}}}\right)^2}} \quad (1)$$

where d_p is the penetration depth, λ the wavelength, and θ the angle of incidence (54.7°). Since the refractive index of Si is 3.44 (n_{Si}) and that of acetonitrile is 1.34 (n_{ACN}), for wavenumbers ranging from 1200 to $3100\ \text{cm}^{-1}$, the penetration depth varies from 535 to 207 nm. This implies that, particularly for the lower IR frequencies, almost the complete volume of the nanofluidic channels is sampled.

Knoevenagel Condensation Reaction. Malononitrile (Sigma Aldrich), *p*-anisaldehyde (Sigma Aldrich), acetonitrile (Sigma Aldrich), DBU (Sigma Aldrich), and 2-[(4-methoxyphenyl) methylidene] propane dinitrile (PMB) (Sigma Aldrich) were used without further treatment. Solutions of 2.7 M, 0.9 M, 0.3 M, 0.1 M, 33 mM, and 11 mM of malononitrile, *p*-anisaldehyde, and DBU in acetonitrile were prepared, and solutions of 0.45 M, 0.135 M, 45 mM, and 15 mM of PMB were prepared. For the reaction studies, 2.7 M malononitrile, 2.7 M *p*-anisaldehyde, and 2.7 M, 0.9 M, 0.3 M, 0.1 M, 33 mM, or 11 mM solutions of DBU were used. Solutions of equal volumes were mixed externally before introduction in the chip. The measurements started exactly 1 min after the solutions were mixed. For each reaction experiment, spectra were recorded every minute, with an integration time of 3 s, up to a total reaction time of 1 h. After each ATR-IR experiment with a specific calibration solution of reaction mixture, the chip was washed with pure acetonitrile and dried in nitrogen flow.

RESULTS AND DISCUSSION

Infrared spectra that were obtained with the device, of the solvent (acetonitrile), and compounds involved in the studied Knoevenagel reaction, viz., malononitrile (main band at $2964\ \text{cm}^{-1}$ ($\nu_{\text{C-H}}$)), *p*-anisaldehyde (main band at $1685\ \text{cm}^{-1}$ ($\nu_{\text{C=O}}$)), DBU (main band at $1616\ \text{cm}^{-1}$ ($\nu_{\text{C=N}}$)), and PMB (main band at $2227\ \text{cm}^{-1}$ ($\nu_{\text{C}\equiv\text{N}}$)), are in good agreement with reference spectra.²¹ Linearity of the measured intensity of the main bands as a function of concentration, as achieved in the device, is excellent (see the Supporting Information). Calibration curves allowed calculation of the concentrations from spectra obtained in the nanofluidic ATR-IR experiments. The conditions applied for the *in situ* study of the reaction were 0.9 M malononitrile, 0.9 M *p*-anisaldehyde, and various concentrations of the catalyst 1,8-diazabicyclo[5.4.0]undec-7-ene (DBU), namely, 0 mM, 4 mM, 11 mM, 33 mM, 0.1 M, 0.3, and 0.9 M. DBU is a strong, non-nucleophilic base, which is frequently used to catalyze condensation reactions. The reactions were all carried out at room temperature ($20\ ^\circ\text{C}$). The resulting spectra at reaction times of 1, 10, 20, 30, and 60 min are shown in Figure 2.

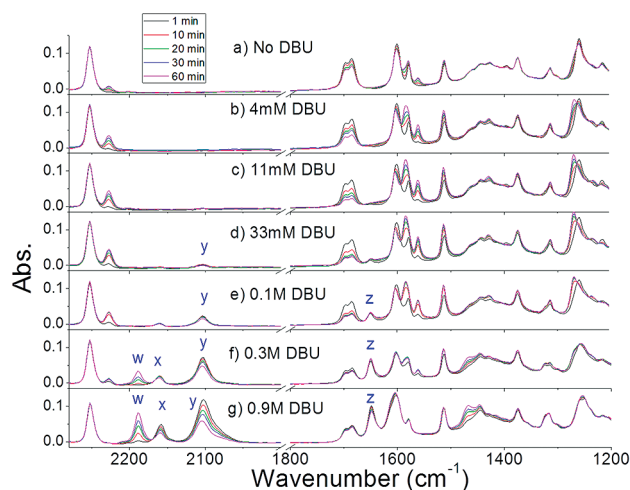


Figure 2. Infrared spectra after 1, 10, 20, 30, and 60 min reaction time, for a reaction involving 0.9 M malononitrile and 0.9 M *p*-anisaldehyde, with different DBU concentrations: (a) no DBU, (b) 4 mM DBU, (c) 11 mM DBU, (d) 33 mM DBU, (e) 0.1 M DBU, (f) 0.3 M DBU, and (g) 0.9 M DBU.

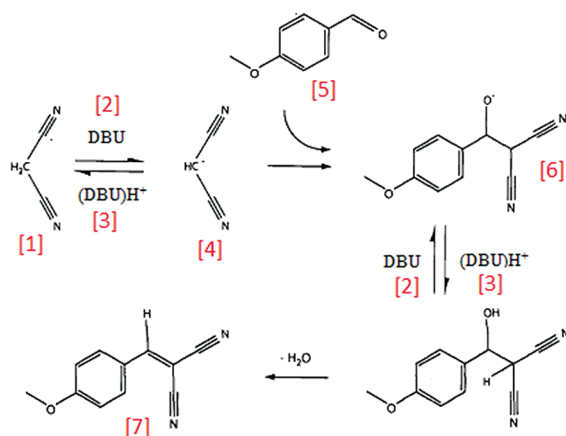
Four unknown infrared bands are observed in the reaction spectra, which could not be assigned to any of the pure compounds. These are indicated in Figure 2 as w ($2188\ \text{cm}^{-1}$), x ($2157\ \text{cm}^{-1}$), y ($2102\ \text{cm}^{-1}$), and z ($1648\ \text{cm}^{-1}$). Note that these bands become more prominent at higher DBU concentrations, and also that for longer reaction times, bands x and y decrease significantly whereas band w increases. Mixtures of malononitrile and DBU were prepared and IR spectra recorded to allow identification of these unknown bands x, y, and z (see the Supporting Information). Our first hypothesis, namely, that these bands are related to a reaction with the silicon surface (e.g., with the silanol groups which are usually present on the surface of silicon²²), was evaluated by repeating some of the experiments with a commercial ZnSe ATR crystal. Again the same bands were observed, suggesting that they are related to reaction intermediates. The malononitrile carbanion, which has been well characterized both experimentally and theoretically,²³ exhibits IR absorptions for $\text{C}\equiv\text{N}$ vibrations at $2158\ \text{cm}^{-1}$ ($\nu_{\text{C}\equiv\text{N}}^{\text{s}}$) and at $2104\ \text{cm}^{-1}$ ($\nu_{\text{C}\equiv\text{N}}^{\text{as}}$)²³ this band is Fermi-split, and the perturbed frequencies are 2115 and $2082\ \text{cm}^{-1}$. These absorptions correspond with bands x and y in our spectra, respectively, which by closer inspection, scale with the DBU concentration. Small deviations between the bands observed by us and those reported in literature are due to the fact that CN vibrations are heavily affected by the local charge.²³ The carbanion participates in the Knoevenagel condensation and is formed due to proton transfer from malononitrile to the strong base DBU (see the Supporting Information).

A possible assignment of the unknown peak z at $1648\ \text{cm}^{-1}$ could be water produced in the reaction. However, when the chip is filled with pure water (55 M), the spectrum shows an absorbance of 0.15 at $1640\ \text{cm}^{-1}$ (Figure SI-8 in the Supporting Information). The intensity observed in Figure 2 would then suggest the presence of as much as 20 M water, which is not realistic in view of the initial concentrations (0.9 M) of reactants. We hypothesize that band z ($1648\ \text{cm}^{-1}$) corresponds to protonated DBU, for which an IR band at $1640\ \text{cm}^{-1}$ was assigned.²⁴ In order to further prove this hypothesis, we performed experiments with different mixtures

of DBU and malononitrile, which demonstrates that band *z* scales with DBU concentration (see the Supporting Information). From this we conclude that band *z* indeed belongs to protonated DBU and most likely corresponds to a C≡N vibration of DBU that shifts from 1614 cm⁻¹ to 1648 cm⁻¹ after protonation.

The remaining unknown band *w* (2188 cm⁻¹) was not observed in spectra of a mixture of *p*-anisaldehyde and DBU (see the Supporting Information); evidently this band is only present in a system containing all three compounds *p*-anisaldehyde, malononitrile, and DBU. Looking at the detailed mechanism of the Knoevenagel condensation in Scheme 2, it is

Scheme 2. Detailed Mechanism of the Knoevenagel Condensation Reaction of Scheme 1



suspected that band *w* belongs to the alkoxide intermediate (marked as chemical 6 in Scheme 2). The observed IR absorption band at 2188 cm⁻¹ would correspond to a C≡N vibration with a slightly charged environment, because C≡N

vibrations without any charge are typically located above 2200 cm⁻¹. A UV–vis spectrum of this solution after 1500 times dilution (see the Supporting Information) was similar to that of PMB, which indicates that the intermediate decomposes to form PMB after dilution.

Figure 3 shows a zoom-in of seven different bands, recorded at different DBU concentrations, and their evolution with reaction time. On the basis of calibration curves, these data have been used to yield the concentration change of PMB with time as presented in Figure 4, which shows the concentration of

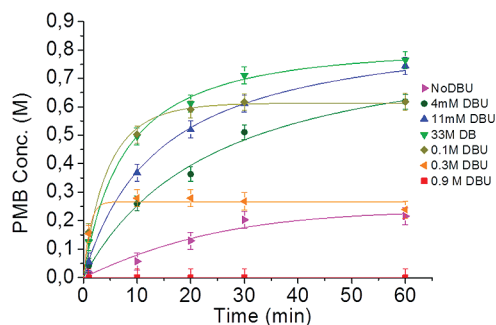


Figure 4. Plot of PMB concentrations measured online during the Knoevenagel condensation and fitted curves for different DBU concentrations.

PMB with different DBU concentrations after 1, 10, 20, 30, and 60 min. The lines in Figure 4 are fitting functions based on the kinetic eq 2,¹⁵ which assumes that the addition of the enolate anion to *p*-anisaldehyde is the rate determining step:

$$C_P = \frac{C_{A0}(e^{(2k_f C_{Ae} C_{A0} / C_{A0} - C_{Ae} t)} - 1)(C_{A0} - C_{Ae})}{C_{A0}(e^{(2k_f C_{Ae} C_{A0} / C_{A0} - C_{Ae} t)} - 1) + 2C_{Ae}} \quad (2)$$

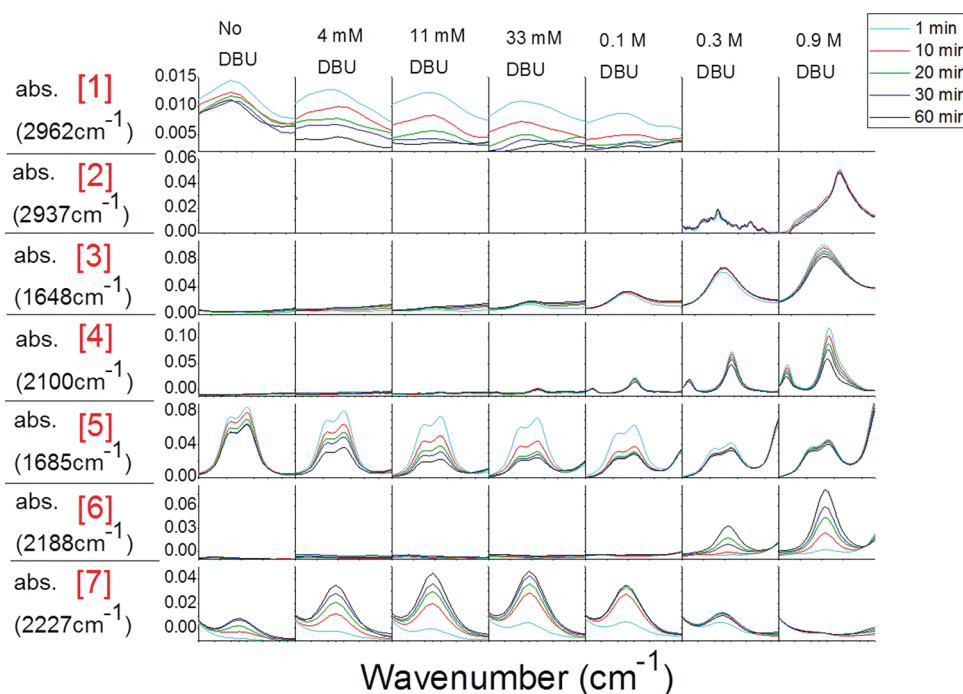


Figure 3. IR spectra of intermediates during the course of a Knoevenagel condensation reaction, numbers correspond to species in Scheme 2. The indicated wavenumber corresponds to the position of the highest intensity.

where C_p is the concentration of product (PMB), C_{A0} the initial concentration of malononitrile or anisaldehyde, C_{Ae} the concentration of malononitrile or anisaldehyde at equilibrium, t the time (in minutes), k_f the forward reaction rate, and k_r the reverse reaction rate, which can be calculated from k_f as $k_r = k_f(C_{Ae}/C_{A0} - C_{Ae})^2$.

The Levenberg-Marquart algorithm was used for fitting Figure 4. Fitting R values are between 0.93 and 0.99. The k_f (forward reaction rate), k_r (reverse reaction rate), and PC_e (PMB concentration at equilibrium) values and their standard errors obtained from the fits are shown in Table 1. Fitted values

Table 1. Values for k_f , k_r , and Percentage Conversion at Equilibrium, From the Fits in Figure 4

C_{cat}^a /mM	k_f^b /(mM min ⁻¹)	k_r^c /(mM min ⁻¹)	PC_e^d /%
0	11 (±1.9)	86 (±1.9)	25.9 (±3.6)
4	43 (±3)	1 (±3)	86.2 (±21)
11	78.4 (±2.2)	2.9×10^{-27} (±2.2)	100 (±5 × 10 ⁻¹²)
33	138 (±10)	2.5 (±10)	88.1 (±4.4)
100	185 (±23)	40.5 (±23)	68.1 (±1.6)
300	251 (±4.5)	1425 (±4.5)	29.6 (±1)
900	0	0	0

^a C_{cat} = catalyst (DBU) concentration. ^b k_f = forward reaction rate constant. ^c k_r = backward reaction rate constant. ^d PC_e = percentage of conversion at equilibrium.

of PC_e show that the product yield at equilibrium increases with DBU concentration until 11 mM DBU and decreases to 0% with 900 mM DBU. We speculate that the dependence of the formation rate of PMB on DBU concentration is due to ionic liquid formation. Indeed it has recently been shown that DBU can form ionic liquids.²⁵ These ionic liquids are usually prepared as a solvent before a chemical reaction, but in our system we believe that the ionic liquid, depending on DBU concentration, is formed during the reaction. Thus, the formation rate of PMB increases with DBU concentration up to 11 mM DBU, while at still higher DBU concentration, intermediates are stabilized by protonated DBU due to the ionic liquid character, which decreases and even stops the production of PMB. To the best of our knowledge, this is the first time that this effect is reported, probably because we are able to study concentrations 3 orders of magnitude higher than was previously feasible. Previous work on this reaction was done at much lower concentrations, mainly in order to stay within the dynamic range of UV–vis spectroscopy,¹⁵ which is not necessary for the present infrared technique.

As a final exercise, we have tested the mechanistic knowledge obtained from the 71 nL nanofluidic sample cell against reaction in a lab scale batch reactor. Solutions with a volume of a few milliliters were prepared with the same concentrations as was done for the nanofluidic chip. Seven different conditions identical to Figure 2 were applied, and the reaction was run in glass containers. The reaction mixture was left for 1 week in a fume hood to evaporate solvent (see the Supporting Information). For conditions a, b, and c (see Figure 2), crystallites of PMB were found. However, for conditions f and g, a dark liquid was observed, which does not solidify or evaporate, even after 1 week. This supports our hypothesis that an ionic liquid is formed, which are known to have very low vapor pressures.

SUMMARY

We have designed and constructed a nanofluidic chip with a reaction volume of only 71 nL, integrated on a silicon ATR-IR crystal with well-defined side faces. Because the nanofluidic channel depth was chosen to match the penetration depth of the ATR evanescent wave, efficient signal acquisition (in terms of signal intensity per sample volume) and low absorbance noise (±0.002) were obtained, and IR spectra could be recorded in a few seconds. With this chip, a Knoevenagel condensation reaction was studied and based on accurate ATR-IR spectra as a function of reaction time, several reaction intermediates were identified, which allowed us to understand details of the reaction mechanism. It was found that two intermediates (alkoxide and carbanion) are stabilized at high catalyst concentration, which we believe is due to an increased ionic liquid character of the solvent. The developed chip will be valuable for *in situ* studies of reaction mechanisms, requiring only limited amounts of scarce or expensive compounds, such as isotopes. Furthermore, it may become useful as an in-line detector for, e.g., capillary-based chromatographic systems¹⁷ which have peak volumes in the range of tens of nanoliters.

ASSOCIATED CONTENT

Supporting Information

Related spectra, calibration spectra, and curves. This material is available free of charge via the Internet at <http://pubs.acs.org>.

AUTHOR INFORMATION

Corresponding Author

*E-mail: e.karabudak@utwente.nl

Notes

The authors declare no competing financial interest.

ACKNOWLEDGMENTS

This research was supported by the Technology Foundation STW, applied science division of NWO, and the technology program of the Ministry of Economic Affairs of The Netherlands, through the “VICI Vernieuwingsimpuls program” (personal grant to H.J.G.E. Gardeniers).

REFERENCES

- (1) Christian, G. D. *Analytical Chemistry*, 6th ed.; John Wiley & Sons, Inc.: Hoboken, NJ, 2004.
- (2) He, H.; Kuo, J. S.; Chiu, D. T. *Appl. Phys. Lett.* **2005**, *87*, 031916.
- (3) Eijkel, J. C. T.; van den Berg, A. *Microfluid. Nanofluid.* **2004**, *1*, 249–267.
- (4) Edel, J. B., deMello, A. J., Eds. *Nanofluidics: Nanoscience and Nanotechnology*; RSC Publishing: Cambridge, U.K., 2008.
- (5) Karnik, R.; Fan, R.; Yue, M.; Li, D. Y.; Yang, P. D.; Majumdar, A. *Nano Lett.* **2005**, *5*, 943–948.
- (6) Schoch, R. B.; Han, J.; Renaud, P. *Rev. Mod. Phys.* **2008**, *80*, 839–883.
- (7) Stuart, B. *Infrared Spectroscopy Fundamentals and Applications*; John Wiley & Sons: Chichester, England, 2004.
- (8) Viganò, C.; Ruyssehaert, J. M.; Goormaghtigh, E. *Talanta* **2005**, *65*, 1132–1142.
- (9) Szafran, M.; Degaszafran, Z. *J. Mol. Struct.* **1994**, *321*, 57–77.
- (10) Herzig-Marx, R.; Queeney, K. T.; Jackman, R. J.; Schmidt, M. A.; Jensen, K. F. *Anal. Chem.* **2004**, *76*, 6476–6483.
- (11) Greener, J.; Abbasi, B.; Kumacheva, E. *Lab Chip* **2010**, *10*, 1561–1566.
- (12) Sarov, Y.; Sarova, V.; Ivanov, Tzv.; Ivanova, K.; Capek, I.; Rangelow, I. W. *Chem. Eng. J.* **2008**, *135*, S284–S287.

- (13) Sarov, Y.; Capek, I.; Ivanov, Tzv.; Ivanova, K.; Sarova, V.; Rangelow, I. W. *Nano Lett.* **2008**, *8*, 375–381.
- (14) Oh, Y. J.; Gamble, T. C.; Leonhardt, D.; Chung, C. H.; Brueck, S. R. J.; Ivory, C. F.; Lopez, G. P.; Petsev, D. N.; Han, S. M. *Lab Chip* **2008**, *8*, 251–258.
- (15) Bula, W. P.; Verboom, W.; Reinhoudt, D. N.; Gardeniers, H. J. G. E. *Lab Chip* **2007**, *7*, 1717–1722.
- (16) Mozharov, S.; Nordon, A.; Littlejohn, D.; Wiles, C.; Watts, P.; Dallin, P.; Girkin, J. M. *J. Am. Chem. Soc.* **2011**, *133*, 3601–3608.
- (17) Kuligowski, J.; Quintás, G.; Garrigues, S.; Lendl, B.; de la Guardia, M.; Lendl, B. *Anal. Chem.* **2010**, *29*, 544–552.
- (18) Ogburn, E. T.; Dziewatkoski, M.; Moles, D.; Johnson, J. M.; Heineman, W. R. *Anal. Chem.* **2011**, *83*, 6963–6970.
- (19) Gardeniers, H. J. G. E. *Anal. Bioanal. Chem.* **2009**, *394*, 385–397.
- (20) Tsukahara, T.; Mawatari, K.; Kitamori, T. *Chem. Soc. Rev.* **2010**, *39*, 1000–1013.
- (21) National Institute of Standards and Technology. *NIST Chemistry WebBook*; 2011.
- (22) Brivio, M.; Oosterbroek, R. E.; Verboom, W.; Goedbloed, M. H.; van den Berg, A.; Reinhoudt, D. N. *Chem. Commun.* **2003**, 1924–1925.
- (23) Binev, Y. I.; Tsenov, J. A.; Juchnovski, I. N.; Binev, I. G. *J. Mol. Struct.: THEOCHEM* **2003**, *625*, 207–214.
- (24) Heldebrant, D. J.; Jessop, P. G.; Thomas, C. A.; Eckert, C. A.; Liotta, C. L. *J. Org. Chem.* **2005**, *70*, 5335–5338.
- (25) Chen, X; Ying, A. In *Ionic Liquids: Applications and Perspectives*; Kokorin, A., Ed.; InTech: Rijeka, Croatia, 2011; <http://www.intechopen.com/articles/show/title/dbu-derived-ionic-liquids-and-their-application-in-organic-synthetic-reactions>.